Control of ionization processes in high band gap materials via tailored femtosecond pulses

L. Englert[1], B. Rethfeld[2], L. Haag[1], M. Wollenhaupt[1], C. Sarpe-Tudoran[1] and T. Baumert[1]

[1] *Institut fuer Physik and CINSaT, Universitaet Kassel, Heinrich-Plett-Str. 40, D-34132 Kassel, Germany*

[2] *Technische Universitaet Kaiserslautern, Erwin-Schroedinger-Strasse 46, D-67663 Kaiserslautern, Germany*

baumert@physik.uni-kassel.de

Abstract: Control of two basic ionization processes in dielectrics i.e. photo ionization and electron–electron impact ionization on intrinsic time and intensity scales is investigated experimentally and theoretically. Temporally asymmetric femtosecond pulses of identical fluence, spectrum and pulse duration result in different final free electron densities. We found that an asymmetric pulse and its time reversed counterpart address two ionization processes in a different fashion. This results in the observation of different thresholds for surface material modification in sapphire and fused silica. We conclude that control of ionization processes with tailored femtosecond pulses is suitable for robust manipulation of breakdown and thus control of the initial steps of laser processing of high band gap materials.

OCIS codes: (140.3390) Laser materials processing; (140.3440) Laser-induced breakdown; (190.4180) Multiphoton processes; (220.4241) Nanostructure fabrication; (320.5540) Pulse shaping; (320.2250) Femtosecond phenomena; (320.7130) Ultrafast processes in condensed matter, including semiconductors.

References and links

1. L. Sudrie, A. Couairon, M. Franco, B. Lamouroux, B. Prade, S. Tzortzakis, and A. Mysyrowicz, "Femtosecond Laser-Induced Damage and Filamentary Propagation in Fused Silica," Phys. Rev. Lett. **89**, 186601 (2002).
2. S. S. Mao, F. Quéré, S. Guizard, X. Mao, R. E. Russo, G. Petite, and P. Martin, "Dynamics of femtosecond laser interactions with dielectrics," Appl. Phys. A **79**, 1695–1709 (2004).
3. A. Vogel and V. Venugopalan, "Mechanisms of pulsed laser ablation of biological tissues," Chem. Rev. **103**, 577–644 (2003).
4. H. Misawa and J. Juodkazis, *3D Laser Microfabrication* (Wiley-VCH, Weinheim, 2006).
5. B. C. Stuart, M. D. Feit, A. M. Rubenchik, B. W. Shore, and M. D. Perry, "Laser-Induced Damage in Dielectrics with Nanosecond to Subpicosecond Pulses," Phys. Rev. Lett. **74**, 2248–2251 (1995).
6. A. C. Tien, S. Backus, H. C. Kapteyn, M. M. Murnane, and G. Mourou, "Short-Pulse Laser Damage in Transparent Materials as a Function of Pulse Duration," Phys. Rev. Lett. **82**, 3883–3886 (1999).
7. M. Lenzner, J. Krüger, S. Sartania, Z. Cheng, C. Spielmann, G. Mourou, W. Kautek, and F. Krausz, "Femtosecond Optical Breakdown in Dielectrics," Phys. Rev. Lett. **80**, 4076–4079 (1998).
8. M. Li, S. Menon, J. P. Nibarger, and G. N. Gibson, "Ultrafast Electron Dynamics in Femtosecond Optical Breakdown of Dielectrics," Phys. Rev. Lett. **82**, 2394–2397 (1999).
9. G. Petite, S. Guizard, P. Martin, and F. Quéré, "Comment on Ultrafast Electron Dynamics in Femtosecond Optical Breakdown of Dielectrics," Phys. Rev. Lett. **83**, 5182–5182 (1999).

#89085 - $15.00 USD Received 26 Oct 2007; revised 7 Dec 2007; accepted 7 Dec 2007; published 14 Dec 2007

10. Y. P. Deng, X. H. Xie, H. Xiong, Y. X. Leng, C. F. Cheng, H. H. Lu, R. X. Li, and Z. Z. Xu, "Optical breakdown for silica and silicon with double femtosecond laser pulses," Opt. Express **13**, 3096–3103 (2005).
11. R. Stoian, M. Boyle, A. Thoss, A. Rosenfeld, G. Korn, and I. V. Hertel, "Dynamic temporal pulse shaping in advanced ultrafast laser material processing," Appl. Phys. A **77**, 265–269 (2003).
12. P. Audebert, Ph. Daguzan, A. Dos Santos, J. C. Gauthier, J. P. Geindre, S. Guizard, G. Hamoniaux, K. Krastev, P. Martin, G. Petite, and A. Antonetti, "Space-Time Observation of an Electron-Gas in SiO_2," Phys. Rev. Lett. **73**, 1990–1993 (1994).
13. V. V. Temnov, K. Sokolowski-Tinten, P. Zhou, A. El-Khamhawy, and D. von der Linde, "Multiphoton Ionization in Dielectrics: Comparison of Circular and Linear Polarization," Phys. Rev. Lett. **97**, 237403 (2006).
14. I. H. Chowdhury, X. Xu, and A. M. Weiner, "Ultrafast double-pulse ablation of fused silica," Appl. Phys. Lett. **86**, 151110 (2005).
15. C. Sarpe-Tudoran, A. Assion, M. Wollenhaupt, M. Winter, and T. Baumert, "Plasma dynamics of water breakdown at a water surface induced by femtosecond laser pulses," Appl. Phys. Lett. **88**, 261109 (2006).
16. L. V. Keldysh, "Ionization in the field of a strong electromagnetic wave," Sov. Phys. JETP **20**, 1307–1314 (1965).
17. L. N. Gaier, M. Lein, M. I. Stockman, G. L. Yudin, P. B. Corkum, M. Y. Ivanov, and P. L. Knight, "Hole-assisted energy deposition in dielectrics and clusters in the multiphoton regime," J. Mod. Opt. **52**, 1019–1030 (2005).
18. B. Rethfeld, "Unified model for the free-electron avalanche in laser-irradiated dielectrics," Phys. Rev. Lett. **92**, 187401 (2004).
19. B. Rethfeld, "Free-electron generation in laser-irradiated dielectrics," Phys. Rev. B **73**, 035101 (2006).
20. E. Louzon, Z. Henis, S. Pecker, Y. Ehrlich, D. Fisher, M. Fraenkel, and A. Ziegler, "Reduction of damage threshold in dielectric materials induced by negatively chirped laser pulses," Appl. Phys. Lett. **87**, 241903 (2005).
21. A. Kaiser, B. Rethfeld, M. Vicanek, and G. Simon, "Microscopic processes in dielectrics under irradiation by subpicosecond laser pulses," Phys. Rev. B **61**, 11437–11450 (2000).
22. A. M. Weiner, "Femtosecond pulse shaping using spatial light modulators," Rev. Sci. Instrum. **71**, 1929–1960 (2000).
23. A. Assion, M. Wollenhaupt, L. Haag, F. Mayorov, C. Sarpe-Tudoran, M. Winter, U. Kutschera, and T. Baumert, "Femtosecond laser-induced breakdown spectrometry for Ca^{2+} analysis of biological samples with high spatial resolution," Appl. Phys. B **77**, 391–397 (2003).
24. M. Gu, *Advanced optical imaging theory* (Springer-Verlag, Berlin, 2000).
25. J. C. Diels and W. Rudolph, *Ultrashort Laser Pulse Phenomena* (Academic Press, 2006).
26. M. Wollenhaupt, A. Assion, and T. Baumert, "Femtosecond Laser Pulses: Linear Properties, Manipulation, Generation and Measurement," in *Handbook of Lasers and Optics*, F. Träger, ed. (Springer, New York, 2007), Chap. 12.
27. A. Präkelt, M. Wollenhaupt, A. Assion, C. Horn, C. Sarpe-Tudoran, M. Winter, and T. Baumert, "Compact, robust and flexible setup for femtosecond pulse shaping," Rev. Sci. Instrum. **74**, 4950–4953 (2003).
28. J. D. McMullen, "Chirped-pulse compression in strongly dispersive media," J. Opt. Soc. Am. **67**, 1575–1578 (1977).
29. L. Englert, M. Wollenhaupt, L. Haag, C. Sarpe-Tudoran, B. Rethfeld, T. Baumert, "Material processing of dielectrics with temporally asymmetric shaped femtosecond laser pulses on the nanometer scale," submitted (2007).
30. L. L. Tatarinova, M. E. Garcia, "Analytical theory for the propagation of laser beams in nonlinear media," Phys. Rev. A **76**, 042824 (2007).
31. G. Heck, J. Sloss, and R. J. Levis, "Adaptive control of the spatial position of white light filaments in an aqueous solution," Opt. Comm. **259** 216–222 (2006).
32. R. Ackermann, E. Salmon, N. Lascoux, J. Kasparian, P. Rohwetter, K. Stelmaszczyk, S. Li, A. Lindinger, L. Wöste, P. Béjot, L. Bonacina, and J.-P. Wolf, "Optimal control of filamentation in air," Appl. Phys. Lett. **89**, 171117 (2006).
33. M. Y. Shverdin, S. N. Goda, G. Y. Yin, and S. E. Harris, "Coherent control of laser-induced breakdown," Opt. Lett. **31**, 1331–1333 (2006).

1. Introduction

Lasers delivering ultrashort pulses have emerged as a unique tool for processing wide band gap materials for a variety of applications ranging from precision micromachining on and below the wavelength of light to new methods of medical surgery (see for example [1, 2, 3, 4] and references therein). Dielectric material, which is transparent for light in the visible and near infrared spectral region, becomes highly absorbing when ultrashort laser pulses of sufficient high intensity are applied. This allows material processing as well as implying the risk of damage of optical components. Effective control of laser induced damage of dielectric material is thus required. One of the key parameters for eventual phase transitions or creation of voids is the

#89085 - $15.00 USD Received 26 Oct 2007; revised 7 Dec 2007; accepted 7 Dec 2007; published 14 Dec 2007

transient free electron density. A large number of experiments has been devoted to the study of laser induced damage of dielectrics as experimental evidence for exceeding a certain critical electron density under laser interaction. These involve pulse duration measurements [5, 6, 7], double pulse experiments [8, 9, 10] and pulse train experiments [11] all showing a strong dependence of the damage threshold on pulse duration and on pulse separation. Direct studies of transient electron densities range from intensities below up to well above the breakdown threshold [2, 12, 13, 14, 15]. These studies show that below the breakdown threshold multiphoton ionization is the main ionization mechanism for ultrashort pulses and that well above the threshold the plasma reflectivity prevents further energy deposition into the material.

In this work we present experimental studies with temporally asymmetric pulse shapes, enabling us to control the temporal evolution of the free electron density. We reveal a systematic dependence of the surface damage threshold on the laser pulse shape for different dielectric materials. Calculations show that the characteristics of the free electron density increase as well as its final value strongly depends on the laser pulse shape.

The free electron density in laser irradiated dielectrics is controlled by the ionization processes transferring electrons from the fully occupied valence band to the initially nearly empty conduction band. For intensities around breakdown threshold mainly two ionization processes are under discussion: photo ionization (i.e. multiphoton ionization which turns for higher intensities to tunnel ionization [16]) and electron–electron impact ionization, creating an electron avalanche. A further mechanism for energy deposition on ultrafast time scales, namely hole assisted field increase, has been discussed recently [17]. The temporal evolution of the free electron density and the role of the fundamental ionization processes are strongly depending on time and intensity [18, 19] as well as on the instantaneous frequency [20]: While photo ionization generates electrons with low kinetic energy in the conduction band, impact ionization requires electrons of high kinetic energy exceeding the band gap energy. Absorption of additional energy from the laser light by intraband absorption proceeds on timescale of a few femtoseconds as the process of Drude absorption involves microscopic collisions on a femtosecond timescale [21]. Therefore temporal pulse tailoring provides a tool to control the two ionization processes on their intrinsic time and intensity scales. To that end we investigate two temporally asymmetric pulse shapes. One shape consists of a strong pulse followed by a train of pulses with falling off intensities. The other shape is the time reversed counterpart and comprises a pulse train with increasing intensities terminated by a strong pulse. In order to minimize dissipative processes we limit the total pulse duration to below 1 ps. As a check experiments are performed on two different dielectrics, i.e. fused silica and sapphire. In sapphire a carrier lifetime in the tens of ps regime has been measured, whereas in fused silica this lifetime is two orders of magnitude smaller (see [2] and references therein). We measure the damage fluence for the two temporally asymmetric pulse shapes in the two materials as a function of the pulse duration and compare the observed trends to calculations based on the multiple rate equation approach [18, 19].

2. Eperimental setup

In our experiment (see Fig. 1) we combine femtosecond pulse shaping techniques [22] with a microscope setup for material processing [23]. Laser pulses with $\Delta t = 35$ fs full width at half maximum (FWHM) pulse duration (measured in the interaction region) and a central wavelength of 790 nm are provided by an amplified Ti:Sapphire laser system. For crosscorrelation measurements the pulses are split into two beams using a Mach–Zehnder interferometer. After passing the interferometer the pulses are focused via a 50x/0.5 objective to a calculated spot diameter of 1.4 μm ($1/e^2$ value of intensity profile) [24]. This value was verified by analyzing laser damage obtained with pulses of 35 fs duration in dielectrics for a fluence well above dam-

#89085 - $15.00 USD Received 26 Oct 2007; revised 7 Dec 2007; accepted 7 Dec 2007; published 14 Dec 2007

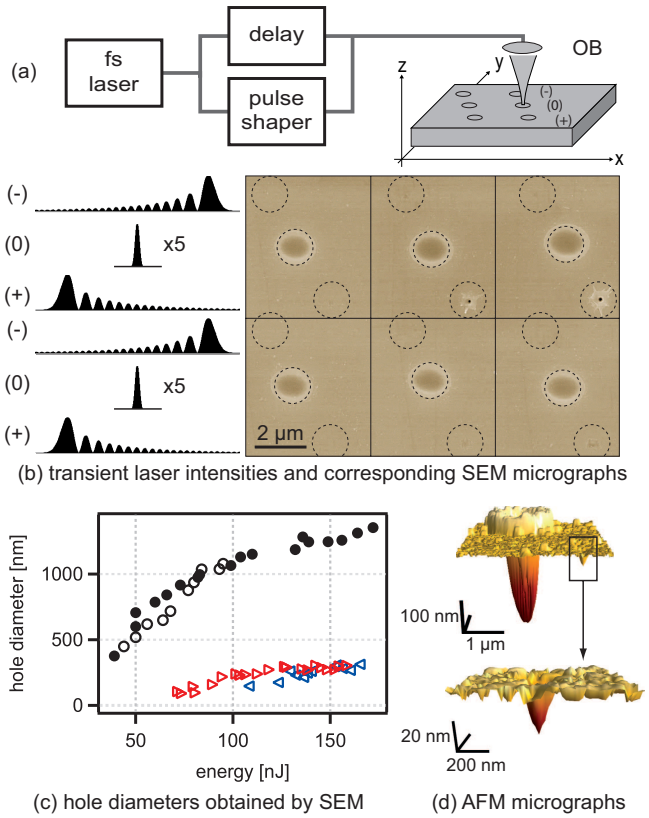

Fig. 1. (Color online) (a) Schematic of experimental set up. For material processing we increase the pulse energy in the x direction in steps of 6 nJ and change the focal z position in the y direction by 1 μm. For each setting we apply three laser pulses, all having the same energy: one with negative cubic phase (-), one unshaped (0) and one with positive cubic phase (+) depicted also by the dotted circles in (b), where they indicate diffraction limit. (b) Transient laser intensities and corresponding SEM micrographs of a subset of laser generated structures in fused silica obtained by the procedure described in (a). Top row: surface in focal plane; lower row: surface 1 μm below focal plane. The large structure in all areas is due to the unshaped pulses (0) and their size is close to the diffraction limit. The appearance of the small structure for positive cubic phase (+) in the middle column defines the threshold for $\phi_3 = +6 \times 10^5$ fs^3. For negative cubic phase $\phi_3 = -6 \times 10^5$ fs^3 (-), i.e. the time reversed pulse, the threshold is not yet reached leaving the surface unaffected. (c) Diameters of ablation structures for fused silica with $\phi_3 = 0$ fs^3 ($\circ$ and $\bullet$ for two independent measurements), for $\phi_3 = +6 \times 10^5$ fs^3 ($\triangleright$) and $\phi_3 = -6 \times 10^5$ fs^3 ($\triangleleft$). Note that the hole diameter obtained with the latter parameters is remarkably robust with respect to variations in laser intensity. (d) Exemplified topology of the large structure (top) due to the unshaped pulse and the small structure (bottom) obtained by the shaped pulse measured via AFM. Note that this small structure is an order of magnitude below the diffraction limit.

#89085 - $15.00 USD Received 26 Oct 2007; revised 7 Dec 2007; accepted 7 Dec 2007; published 14 Dec 2007

age threshold. The calculated axial dimension of the $1/e^2$ intensity point spread function in air is 9.1 μm. For temporal pulse diagnostics a two–photon photodiode is placed in the interaction region. By applying 2^{nd} and 3^{rd} order polynominal spectral phase functions [25, 26] to our calibrated home built phase modulator [27] we confirmed a flat phase in the interaction region. Shaped pulses are characterized by the implemented phase functions occasionally checked via direct crosscorrelation measurements. Crosscorrelations for different cubic phase parameters (3^{rd} order polynominal spectral phase) are shown in Fig. 2. Direct measured crosscorrelations are in agreement with numerical simulations. Analytic formulas for cubic phase shaped laser pulses of the form $\phi(\omega) = \frac{\phi_3}{3!} \cdot (\omega - \omega_0)^3$ can be found in [26, 28]. In our case the 2σ pulse duration [25] increases from 85 fs at $\phi_3 = +5 \times 10^4$ fs^3 to 960 fs at $\phi_3 = +6 \times 10^5$ fs^3 approximately linearly in ϕ_3 [26]. For material processing phase shaped femtosecond pulses are

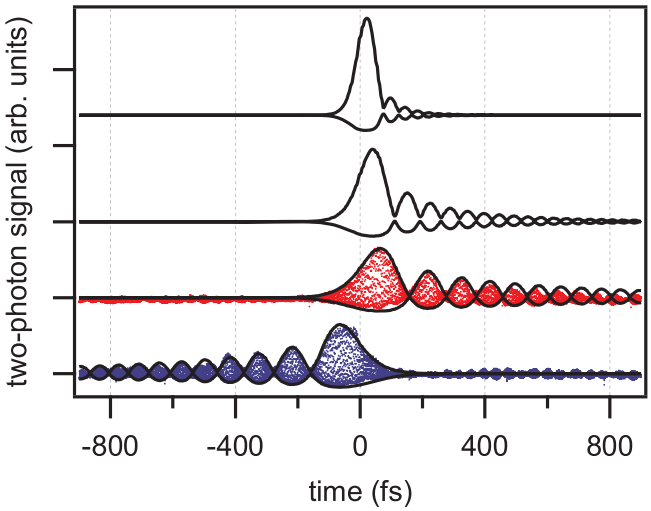

Fig. 2. (Color online) Comparison of measured and calculated crosscorrelation between bandwidth limited 35 fs pulses and third order dispersion shaped pulses. Envelopes are shown as solid lines for different cubic phase masks. From top to bottom: $\phi_3 = +5 \times 10^4$ fs^3, $+2 \times 10^5$ fs^3 and $+6 \times 10^5$ fs^3 (red: measured values). The bottom plot shows a negative mask of -6×10^5 fs^3 (blue: measured values).

focused onto fused silica and synthetic sapphire. The single shot pulse energy is adjusted by a motor driven gradient neutral density filter and recorded with a calibrated photodiode. The sample is translated by a 3-axis piezo table to a new position for each shot. In order to ensure that the surface is within our measurement range, we probe the sample surface with a HeNe laser prior to material processing. In a typical measurement pattern (see Fig. 1) we vary the spectral phase mask, energy and focal z-position. The threshold for material damage is determined visually from the scanning electron microscopy (SEM) images (see Fig. 1(b)).

3. Results and discussion

The observed thresholds as a function of the cubic phase parameter are displayed in Fig. 3 for sapphire (left) and fused silica (right). Error bars result from uncertainties in the single shot energy measurements and from visual damage classification. In both material systems we observe the expected increase of the damage threshold energy due to the decrease of intensity caused by the increase of cubic phase.

For vanishing cubic phase the damage threshold of the bandwidth limited pulse is obtained.

#89085 - $15.00 USD Received 26 Oct 2007; revised 7 Dec 2007; accepted 7 Dec 2007; published 14 Dec 2007

The observed threshold fluences of 2.3 J/cm^2 (fused silica) and 2.8 J/cm^2 (sapphire) are consistent with the values reported in the literature [5, 6, 7, 8, 10, 13]. Comparing thresholds for positive and negative cubic phase parameters we find in both materials that the threshold for positive cubic phase is always lower than for negative cubic phase for same absolute value of cubic phase. As the pulses have identical fluence, spectrum and pulse duration we conclude that the *different asymmetric temporal shape, i. e. the energy distribution in time* has a significant influence on the material damage threshold. Additionally the shape and size of the created structures change. Figure 1(b) compares SEM images for bandwidth limited pulses to pulses with positive cubic phase ($+6\times10^5$ fs^3) at the threshold energy (75 ± 9) nJ of the shaped pulse. We observe up to an order of magnitude reduction in the structure diameter (down to 100 nm for pulses with $\phi_3 = +6\times10^5$ fs^3). The topology of the structures is exemplified in Fig. 1(d) with the help of atomic force microscope images. These small structures obtained with cubic phase masks are remarkably stable with respect to variations in laser intensity, whereas the structures for the bandwidth limited pulse shows the known expansion in structure size with increasing laser fluence (see Fig. 1(c)). We attribute this above threshold observation to propagation effects in combination with energy transfer to the lattice and eventual phase transitions or the creation of voids. These effects have not been unraveled so far for temporally asymmetric shaped laser pulses [29]. Recently progress has been made in the development of an analytical theory for the propagation of laser beams in nonlinear media [30] that has the perspective to include temporally shaped femtosecond pulses for the investigation of propagation effects. Within this context experimental control of filamentation processes in water [31] and air [32] as well as laser-induced breakdown in nobel gases [33] with shaped femtosecond laser pulses has been reported. Here we discuss the difference in threshold energies for different signs of

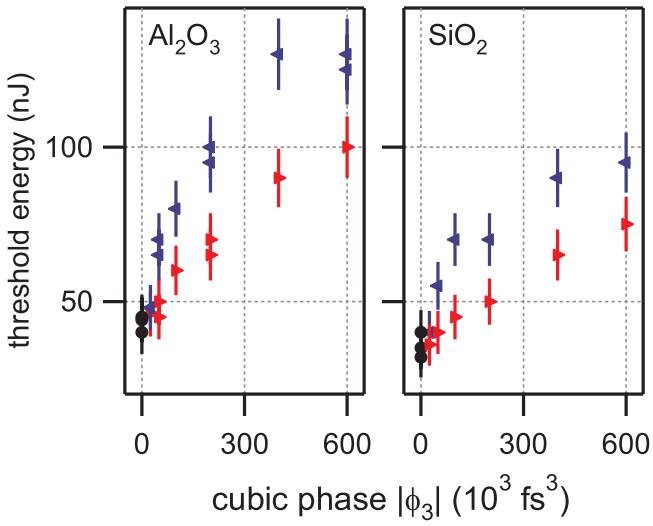

Fig. 3. (Color online) Experimental material processing threshold for sapphire (left) and fused silica (right) for different cubic phase parameters (► for positive ϕ_3, ◄ for negative ϕ_3 and • for unmodulated pulses). Close-by symbols confirm good reproducibility of the measured threshold energies.

the cubic phase i.e. different asymmetric temporal pulse shapes. To that end we calculate the transient free electron density in laser irradiated dielectrics by making use of the multiple rate equation (MRE) [18]. The achievement of a certain critical density is commonly accepted as a criterion for laser induced damage in dielectrics. In the following a remarkable difference in

#89085 - $15.00 USD Received 26 Oct 2007; revised 7 Dec 2007; accepted 7 Dec 2007; published 14 Dec 2007

the transient electron density as well as in its final values is revealed for both signs of phase modulation.

In the calculations we apply material parameters of fused silica and laser parameters as used in the experiments. The photo ionization probability is taken from Ref. [13] as $\sigma_6^{\mathrm{lin}} = 7.5 \times 10^{-47}$ cm^9/sW^6. The probability for intraband absorption for a laser wavelength of $\lambda = 790$ nm is assumed as $W_{1\mathrm{pt}} = 1.38 \times 10^{-6}\ E_L^2$ m^2/V^{2}s, using the value in Ref. [18] and the Drude formula. Recombination (see [2]) is neglected for the present study. Figure 4 shows the increase of total free electron density for negative and positive cubic phase. The corresponding asymmetric temporal intensity profiles are shown as dashed-dotted curves. Here, a pulse dura-

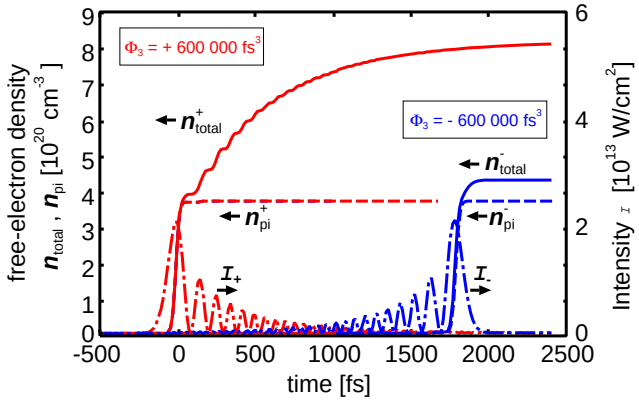

Fig. 4. (Color online) Transient free electron density n_{total} (solid lines) as calculated with help of the MRE, together with the density of electrons provided by photo ionization n_{pi} (dashed lines) and the corresponding transient intensities (dashed-dotted lines) of the positive modulated pulse (red curves, index +) and the negative modulated pulse (blue curves, index -), respectively. The fluence (i.e. the integrated intensity) for these pulse parameters is set to 5 J/cm^2.

tion of $\Delta t = 35$ fs of the unperturbed pulse (FWHM) and a cubic phase with $|\phi_3| = 6 \times 10^5$ fs^3 were applied, resulting in a statistical pulse duration of $2\sigma = 960$ fs. The resulting transient intensity is plotted for the case of $\phi_3 > 0$ and $\phi_3 < 0$. The latter is offset by 4σ in time for better visualization. In both cases, the density of electrons shifted to the conduction band by the process of photo ionization n_{pi} is plotted additionally to the total free electron density n_{total}. For positive cubic phase the total free electron density increases strongly at the beginning of irradiation. Later on, a further gradual increase is observed, attenuating at the end of the laser pulse. In contrast, for the negative cubic phase, the total free electron density increases only by the end of irradiation, when the peak intensity of the pulse train is reached. The final value is lower than for the case of positive cubic phase. This behavior is caused by the strong intensity-dependence of both ionization processes together with their intrinsic time scales. Photo ionization depends on intensity as I^N in case of N-photon ionization. Therefore nearly all electrons are shifted to the conduction band during the peak intensity, reached at the beginning or at the end of irradiation, for the positive and negative cubic phase, respectively. For positive cubic phase, irradiation continues after the peak intensity, thus, the initially provided free electrons are further heated and impact ionization becomes possible. The Drude-like heating of free electrons depends linearly on intensity and the probability of impact ionization depends in turn on the heating process (in the asymptotic long-time regime, impact ionization leads to an exponential increase of free electron density [18, 19]). In this way the intensity dependence of impact ionization is involved. In case of negative cubic phase, the gradually increasing intensity in the

#89085 - $15.00 USD Received 26 Oct 2007; revised 7 Dec 2007; accepted 7 Dec 2007; published 14 Dec 2007

initial phase of the modulated pulse does not provide enough electrons through multiphoton ionization to enable impact ionization. Primarily during the main peak at the *end* of the pulse train, photo ionization becomes important, providing finally the same amount of free electrons n_{pi}^{-} as in the case of a positive phase mask and only a small amount of free electrons is provided by impact ionization.

4. Conclusion

In conclusion we have demonstrated that via temporal asymmetric pulse shapes on intrinsic time and intensity scales, different physical contributions to the free electron density increase can be addressed in high band gap materials. Femtosecond pulse tailoring thus provides a possibility to control the transient free electron density until the critical density for dielectric breakdown is reached. This opens the route to develop tailored pulse shapes for controlled nanoscale material laser processing of dielectrics.

Acknowledgments

This work was supported by the DFG via SPP 1139. We thank T. Weis (Ehresmann group) and R. Krelaus (Schmidt group) for help in obtaining the AFM images.

#89085 - $15.00 USD Received 26 Oct 2007; revised 7 Dec 2007; accepted 7 Dec 2007; published 14 Dec 2007